Brain (2001), **124,** 1100–1113

Skeletal muscle disuse induces fibre type-dependent enhancement of Na^+ channel expression

Jean-François Desaphy,[1] Sabata Pierno,[1] Claude Léoty,[2] Alfred L. George, Jr,[3] Annamaria De Luca[1] and Diana Conte Camerino[1]

[1]*Unit of Pharmacology, Department of Pharmaco-Biology, School of Pharmacy, University of Bari, Italy,* [2]*Laboratory of General Physiology, Faculty of Sciences and Techniques, University of Nantes, France and* [3]*Division of Genetic Medicine, Department of Pharmacology, Vanderbilt University Medical Center, Nashville, Tennessee, USA*

Correspondence to: Professor Diana Conte Camerino, Department of Pharmaco-Biology, School of Pharmacy, University of Bari, Via Orabona, 4 campus, 70125 Bari, Italy
E-mail: conte@farmbiol.uniba.it

Summary

Slow-twitch and fast-twitch muscle fibres have specific contractile properties to respond to specific needs. Since sodium current density is higher in fast-twitch than in slow-twitch fibres, sodium channels contribute to the phenotypic feature of myofibres. Phenotype determination is not irreversible: after periods of rat hindlimb unloading (HU), a model of hypogravity, a slow-to-fast transition occurs together with atrophy in the antigravity slow-twitch soleus muscle. Using cell-attached patch-clamp and northern blot analyses, we looked at sodium channel expression in soleus muscles after 1–3 weeks of HU in rats. We found that sodium channels in fast-twitch flexor digitorum brevis muscle fibres, soleus muscle fibres and 1- to 3-week HU soleus muscle fibres showed no difference in unitary conductance, open probability and voltage-dependencies of activation, fast inactivation and slow inactivation. However, muscle disuse increased sodium current density in soleus muscle fibres 2-fold, 2.5-fold and 3-fold after 1, 2 and 3 weeks of HU, respectively. The concentration of mRNA for the skeletal muscle sodium channel α subunit increased 2-fold after 1 week of HU but returned to the control level after 3 weeks of HU. In contrast, the concentration of mRNA for the ubiquitous sodium channel β_1 subunit was unchanged after 1 week and had increased by 30% after 3 weeks of HU. The tetrodotoxin sensitivity of sodium currents in 3-week HU soleus muscles and the lack of mRNA signal for the juvenile skeletal muscle sodium channel α subunit excluded denervation in our experiments. The observed increase in sodium current density may reduce the resistance to fatigue of antigravity muscle fibres, an effect that may contribute to muscle impairment in humans after space flight or after long immobilization.

Keywords: Na^+ channel; fast and slow skeletal muscles; patch clamp; rat hindlimb unloading; muscle disuse

Abbreviations: FDB = flexor digitorum brevis; HU = hindlimb unloading

Introduction

During development, skeletal muscle fibres evolve into slow- and fast-twitch fibres according to their speed of contraction. All slow-twitch muscle fibres express the type I myosin heavy-chain protein, whereas fast-twitch muscle fibres can be further subdivided into three phenotypes (types IIA, IIB and IIX) according to the myosin heavy-chain protein isoform they express (Schiaffino and Reggiani, 1996). Nevertheless, phenotype determination is not completely irreversible. Adult skeletal muscle fibres can change their phenotype in response to modified functional requests by expressing specific forms or levels of proteins involved in calcium handling, energy metabolism and contractile machinery. For example, it is now well established that fast muscle fibres submitted to chronic low-frequency electrical input acquire many, although not all, of the properties of slow-twitch muscle fibres (Pette and Vrbovà, 1992; Buonanno and Fields, 1999). The inverse transition, i.e. slow to fast, has also been observed in response to unweighting of the antigravity slow-twitch muscles, as in the model of rat hindlimb suspension (Talmadge, 2000). This model, first developed for the study of the effects of microgravity on bone function (Morey, 1979), has been used widely to study skeletal muscle plasticity, showing that fibre type transition induced by muscle disuse is associated with changes in transcript levels for a number of proteins involved in muscle function.

The expression of voltage-gated sodium channels also

differs between slow- and fast-twitch muscle fibres (Milton *et al.*, 1992; Ruff, 1992). Because these channels are of major importance in determining the upstroke as well as the refractory period of the action potential, the density of available sodium channels in the sarcolemma greatly influences the firing pattern of muscle fibres, which in turn contributes to the phenotypic feature of myofibres. Measured with the loose-patch voltage-clamp technique, sodium current density at the end-plate or in the extrajunctional sarcolemma of fast-twitch muscle fibres appears far larger than in slow-twitch muscle fibres (Milton *et al.*, 1992; Ruff, 1992; Ruff and Whittlesey, 1993*a*). This difference depends, at least in part, on the activity of the motor neurone, because transplantation of a fast motor neurone on to a slow muscle increases sodium current density (Milton and Behforouz, 1995). However, the degree to which such a change can occur in pathophysiological situations and the level of channel expression at which it is regulated is not known.

In the present study, we looked at the effects of muscle disuse on the expression of sodium channels in myofibres of the slow-twitch soleus muscle after periods of muscle unweighting obtained using the model of rat hindlimb unloading (HU). Using the patch-clamp technique and molecular biology, we found that muscle disuse increases sodium current density in the extrajunctional sarcolemma of soleus muscle fibres by modifying the levels of transcription of sodium channel α and β_1 subunits in a complex time-dependent manner.

Material and methods

Animal care and surgery

Male Wistar rats (body weight 250–350 g, age 2–3 months) were purchased from Charles River (Calco, Italy) and placed in single cages in sterile housing. Experiments were conducted in accordance with the Italian guidelines for the use of laboratory animals, which conform with the European Community Directive published in 1986 (86/609/EEC). From the rats that were available, animals were selected randomly to be suspended for 1–3 weeks in special cages, as described below (Morey, 1979). The animal was placed in a harness to which was attached one end of a shoelace; the other end of the lace was fixed to a trolley that could move freely on horizontal rails at the top of the cage. The length of the lace was adjusted to allow the forelimbs of the rat to touch the bottom of the cage while the hind limbs were free; the animal's body was inclined at about 45° from the horizontal. The remaining animals (controls) were not suspended. Control and suspended animals had food and water *ad libitum*. At the end of the period of suspension (0–3 weeks), muscles were immediately removed from the animal under deep anaesthesia induced by intraperitoneal injection of urethane (1.2 g/kg body weight). The fast-twitch flexor digitorum brevis (FDB) muscle from the hind foot and the slow-twitch soleus muscle were used for voltage-clamp and molecular studies. At the end of the surgical intervention, animals were killed by an overdose of urethane or by decapitation.

Well-known effects of suspension, e.g. atrophy and the slow-to-fast fibre phenotype transition, were verified on soleus muscles removed from rats that had been suspended for 1 or 3 weeks (S. Pierno, J.-F. Desaphy, A. Frigeri, G. P. Nicchia, M. Svelto, A. De Luca and D. Conte Camerino, unpublished observations). Compared with control animals, the muscle-to-body weight ratio was reduced by ~17 and ~39% after 1 week and 3 weeks of suspension, respectively. Thus, atrophy developed gradually during the period of suspension. Immunofluorescence measurements on soleus muscle cryosections using a specific antibody against the type IIa myosin heavy chain isoform revealed an increment in fast muscle fibre from about 15% of total fibre in control muscle to ~35% after 1 or 3 weeks of suspension. Thus, partial slow-to-fast transition occurred during suspension.

Patch voltage-clamp studies

FDB and soleus muscles removed from control and suspended rats were placed immediately in physiological solution (107.7 mM NaCl, 3.5 mM KCl, 0.7 mM $MgSO_4$, 1.6 mM $CaCl_2$, 26.2 mM $NaHCO_3$, 1.7 mM NaH_2PO_4, 9.6 mM Na-gluconate, 5.5 mM glucose, 7.6 mM sucrose, pH 7.3) supplemented with 3.0 mg/ml collagenase (3.3 IU/ml, type XI-S; Sigma, St Louis, Mo., USA). The preparations were shaken at 70/min for 1–2 h at 32°C under a 95% oxygen/5% carbon dioxide atmosphere. During this incubation period, dissociated cells were sampled and rinsed several times with bath recording solution before being transferred to an RC-11 recording chamber (Warner Instrument, Hamden, Conn., USA).

Sodium currents were recorded at room temperature (21 ± 2°C) in the cell-attached configuration of the patch-clamp method (Hamill *et al.*, 1981) with an AxoPatch 1D amplifier and a CV-4-0.1/100U headstage (Axon Instruments, Foster City, Calif., USA). Pipettes were formed from Corning 7052 glass (Garner Glass, Claremont, Calif., USA) with a vertical puller (PP-82; Narishighe, Tokyo, Japan). They were coated with Sylgard 184 (Dow Corning, Midland, Mich., USA) and heat-polished on a microforge (MF-83; Narishighe). Pipettes had resistances ranging from 2 to 4 MΩ when filled with the recording pipette solution [150 mM NaCl, 1 mM $MgCl_2$, 1 mM $CaCl_2$, 10 mM HEPES (4-(2-hydroxyethyl)-1-piperazine-ethanesulphonic acid), pH 7.3]. Voltage-clamp protocols and data acquisition were performed with pClamp 6.0 software (Axon Instruments) through a 12-bit A–D/D–A interface (Digidata 1200; Axon Instruments). Currents were low-pass filtered at 2 kHz (–3 dB) with the amplifier's four-pole Bessel filter and digitized at 10–20 kHz.

Because sodium channel density is 5- to 10-fold higher on the end-plate border than away from the end-plate (Ruff, 1992), the sodium currents were recorded from the extra-junctional membrane at a site >200 μm from the end-plate,

as described previously (Desaphy *et al.*, 1998*b*). The end-plates were visualized with phase contrast under the ×320 inverted microscope (Axiovert 100; Zeiss) and only fibres with visible end-plates were patched. A recording bath solution containing Cs^+ ions as the main cation (145 mM CsCl, 5 mM EGTA [ethylene glycol-bis(β-aminoethylether)-*N*,*N*,*N*′,*N*′-tetra-acetic acid], 1 mM $MgCl_2$, 10 mM HEPES, 5 mM glucose, pH 7.3) was used in order to inhibit potassium currents and to depolarize the fibre plasma membrane. After 5–10 min of incubation in this solution, the intrinsic resting membrane potential (V_m) of the FDB muscle fibres is consistently close to –5 mV (Desaphy *et al.*, 1998*a*). During the present study, we found no obvious differences from this value for the fibres isolated from soleus muscles. The values of potential given here are those held by the patch-clamp amplifier and are not corrected from V_m.

Membrane passive responses were controlled during the experiments, and the patches in which eventual change might have modified the sodium current characteristics were ignored. Capacitance currents were cancelled almost totally by the compensation circuit of the amplifier. To further eliminate residual capacitance transient and leak current, the scaled passive ensemble average current recorded on return to the holding potential was subtracted from the current traces elicited by the depolarizing pulse (Desaphy *et al.*, 1998*a*).

Specific voltage-clamp protocols applied to the patch membrane for the measure of the current–voltage relationship and the voltage dependence of fast and slow steady-state inactivation are described in the Results section. These protocols were repeated five times for each patch and peak current amplitudes were averaged to obtain reliable values. The steady-state fast inactivation relationships were fitted with the Boltzmann equation $I = I_{max}/\{1 + \exp[(V - V_{1/2})/K]\}$, where I is current, I_{max} is the maximal current, K is the slope factor and $V_{1/2}$ is the potential for having half of the channels inactivated. To describe the voltage dependence of slow inactivation, a non-zero residual current, I_{min}, was included into the Boltzmann equation: $I = I_{min} + (I_{max} - I_{min})/\{1 + \exp[(V- V_{1/2})/K]$. Although a single fit to the data averaged from n patches is presented in the figures, fits were performed for each individual patch to obtain values of standard error of the mean for statistical comparison of the fit parameters between muscle types and animal groups. All average results are reported as the mean and standard error of the mean for n patches. Statistical analysis was performed with Student's t test for paired or grouped data, considering $P < 0.05$ as significant.

Northern blot analysis of sodium channel messengers

Soleus muscles removed from control and suspended rats were frozen immediately in liquid nitrogen. Total RNA was isolated from muscles with a modified acid–phenol method (Chomczynski and Sacchi, 1987). Samples of total RNA (10 µg) were size-fractionated on denaturing 1% agarose/6% formaldehyde (v/v) gels and transferred to a nylon membrane (Hybond-N; Amersham), as described previously (Makita *et al.*, 1994; Pierno *et al.*, 1999). Northern blots were hybridized sequentially with different radiolabelled probes: a rat sodium channel β_1 subunit cDNA probe and two rat sodium channel α subunit antisense RNA probes (SkM1 or SkM2). An 18 S ribosomal RNA radiolabelled probe was used as internal reference in order to establish the relative amount of RNA in each sample. The cDNA probe [1.3 kilobases (kb)] corresponding to the complete coding region and partial 3′-UTR (untranslated region) of the rat β_1 subunit was prepared as described previously (Makita *et al.*, 1994). This probe should have been able to detect messenger RNAs of both β_1 and the recently described splice variant β_1A (Kazen-Gillespie *et al.*, 2000). The β_1 cDNA probe was radiolabelled with [^{32}P]dCTP (cytidine 5′-triphosphate) by use of the random priming method. Hybridization was performed at 42°C for 16 h in a solution containing 50% formamide, 5 × SSPE [1 × SSPE is 0.18 M NaCl, 10 mM Na_2HPO_4, 1 mM EDTA (ethylenediamine tetraacetate)], 1% SDS (sodium dodecyl sulphate), 0.05 M Tris–HCl, pH 7.5, 5 mM EDTA, 1% bovine serum albumin and 1×10^{-6} c.p.m./ml ^{32}P-labelled cDNA probe. Blots were washed with a final stringency of 65°C in 0.1 × SSC, 0.1% SDS after hybridization with cDNA probe. Two plasmids (pSkM1–3UTR, pSkM2–3UTR) were prepared in Bluescript to generate antisense RNA probes from the 3′-UTR of rat SkM1 (nucleotides 5968–6555 of the sequence of GenBank M26643), and the 3′-UTR of rat SkM2 (nucleotides 6509–7076 of the sequence of GenBank L11243). Antisense riboprobe for rat SkM1 was transcribed from *Not*I linearized pSkM1–3UTR using T3 RNA polymerase in the presence of [^{32}P]CTP. Similarly, antisense rat SkM2 was transcribed from *Hin*dIII linearized pSkM2–3UTR using T7 RNA polymerase. Hybridizations were performed at 65°C for 16 h in the same hybridization solution and 2×10^{-6} c.p.m./ml ^{32}P-labelled RNA probe. Blots were washed with a final stringency of 75°C in 0.1 × SSC, 0.1% SDS after hybridization. An 18 S ribosomal RNA radiolabelled probe was used as internal reference in order to establish the relative amount of RNA in each sample. The radiolabelled 18 S RNA riboprobe was synthesized by *in vitro* transcription using an antisense control template (Ambion, Austin, Tex., USA), T7 RNA polymerase and [^{32}P]CTP. Hybridization with 18 S riboprobe was performed at 60°C with 0.5×10^{-6} c.p.m./ml ^{32}P-labelled probe in the hybridization solution, followed by washes in 0.1 × SSC, 0.1% SDS at 68°C. Hybridizing bands were visualized and quantified by phosphor image analysis using ImageQuant software (Molecular Dynamics, Sunnyvale, Calif., USA).

Results

Effect of hindlimb unloading on Na^+ currents

Tens of sodium channels were present in cell-attached patches performed on extrajunctional sarcolemma of freshly

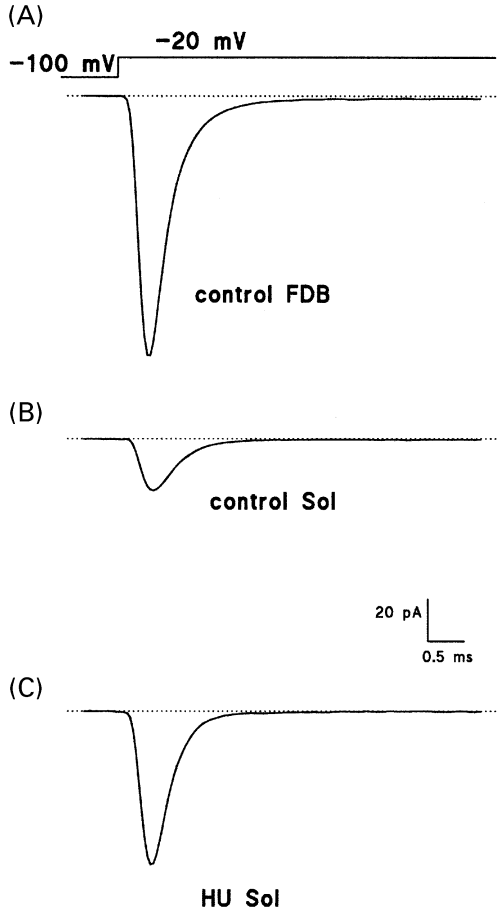

Fig. 1 Hindlimb unloading (HU) increases sodium currents in soleus (Sol) muscle fibres. Na^+ current traces from representative control FDB (**A**), control soleus (**B**) and 3-week HU soleus (**C**) muscle fibres are shown. All three cell-attached macropatches were performed using pipettes with resistance 3.3 MΩ. The currents were elicited by depolarizing the patch membrane from –100 to –20 mV.

dissociated rat skeletal muscle fibres, which allowed recording of macroscopic-current-like sodium currents by depolarizing the patch membrane from a holding potential of –100 mV to a test potential of –20 mV (Fig. 1). The first observation was the difference in current amplitude between control fast- and slow-twitch muscle fibres. In soleus fibres, peak current amplitude ranged from –18.0 to –37.6 pA (n = 12), whereas in FDB fibres it ranged from –42.3 to –172.0 pA (n = 9). Because current amplitude depends on the area of membrane under the patch electrode, we also calculated sodium current density by dividing current amplitude values by the square of the pipette conductance, which was assumed to be linearly correlated to the patch area (Sakmann and Neher, 1983; Desaphy *et al.*, 1998*b*, *c*). The average data presented in Table 1 show significant differences between control soleus and FDB fibres. After 3 weeks of HU, peak current amplitude remained unchanged in FDB muscle fibres (Table 1). In contrast, HU resulted in a significant increase in peak current amplitude in soleus muscle fibres, which ranged from –22.3 to –149.7 pA (Fig. 1). Nevertheless, sodium currents

Table 1 *Peak amplitude and density of sodium currents elicited from –100 to –20 mV in fast- and slow-twitch muscle fibres in control rats and rats that had been subjected to 3 weeks of hindlimb unloading (HU)*

	Peak amplitude (pA)	Density (pA/arbitrary unit)
Control FDB (n = 9)	–106.3 ± 16.4*	–1086 ± 180*
Control soleus (n = 12)	–27.7 ± 2.1	–313 ± 27
HU FDB (n = 6)	–93.5 ± 7.1*	–914 ± 142**
HU soleus (n = 14)	–68.3 ± 11.5*	–673 ± 94*

Sodium currents were elicited by depolarizing the cell-attached patch membrane from –100 to –20 mV. Sodium current density at –20 mV was calculated by dividing the peak current amplitude by the square of the pipette conductance. Data are mean ± standard error of the mean for n patches. *$P < 0.005$ and **$P < 0.01$ versus control soleus muscle fibres, as determined by unpaired Student's t test.

Table 2 *Kinetic parameters of ensemble average sodium currents elicited at –20 mV in fast- and slow-twitch muscle fibres in control rats and rats that had been subjected to 3 weeks of hindlimb unloading (HU)*

	Time to peak (ms)	Inactivation time constant (ms)
Control FDB (n = 9)	0.47 ± 0.02	0.33 ± 0.03
Control soleus (n = 7)	0.44 ± 0.02	0.28 ± 0.02
HU FDB (n = 6)	0.47 ± 0.01	0.34 ± 0.02
HU soleus (n = 13)	0.45 ± 0.01	0.31 ± 0.02

Ensemble average sodium currents were constructed from at least 40 current records elicited by depolarizing the cell-attached patch membrane from –100 to –20 mV. The time to peak was measured as the interval between the initiation of the depolarizing pulse and the peak current amplitude. The inactivation time constant τ was calculated from the fit of the current decay with a monoexponential function of the form $I(t) = A \exp[-t/(\tau)]$. Data are mean ± standard error of the mean for n patches. No significant difference was found between muscle types (Student's grouped t test).

presented very similar kinetics of activation and inactivation in all the experimental conditions, as determined by the time to peak and the current decay exponential time constant (Table 2).

Differences in current amplitude can result from differences in single-channel current, in channel open probability and in the number of channels available. Single-channel current traces typical of soleus muscle fibres of control and 3-week HU rats are illustrated in Fig. 2. Single-channel currents recorded in cell-attached patches of control rat FDB muscles were illustrated in previous studies (Desaphy *et al.*, 1998*a*, *c*). No difference was found in single-channel current amplitude and single-channel conductance between the slow- and fast-twitch fibres (Fig. 2B). Also, HU did not induce any change in these parameters (Fig. 2B). The open probability of sodium channels was calculated by dividing the peak amplitude ($P_{o,max}$) or time integral (P_o) of ensemble average

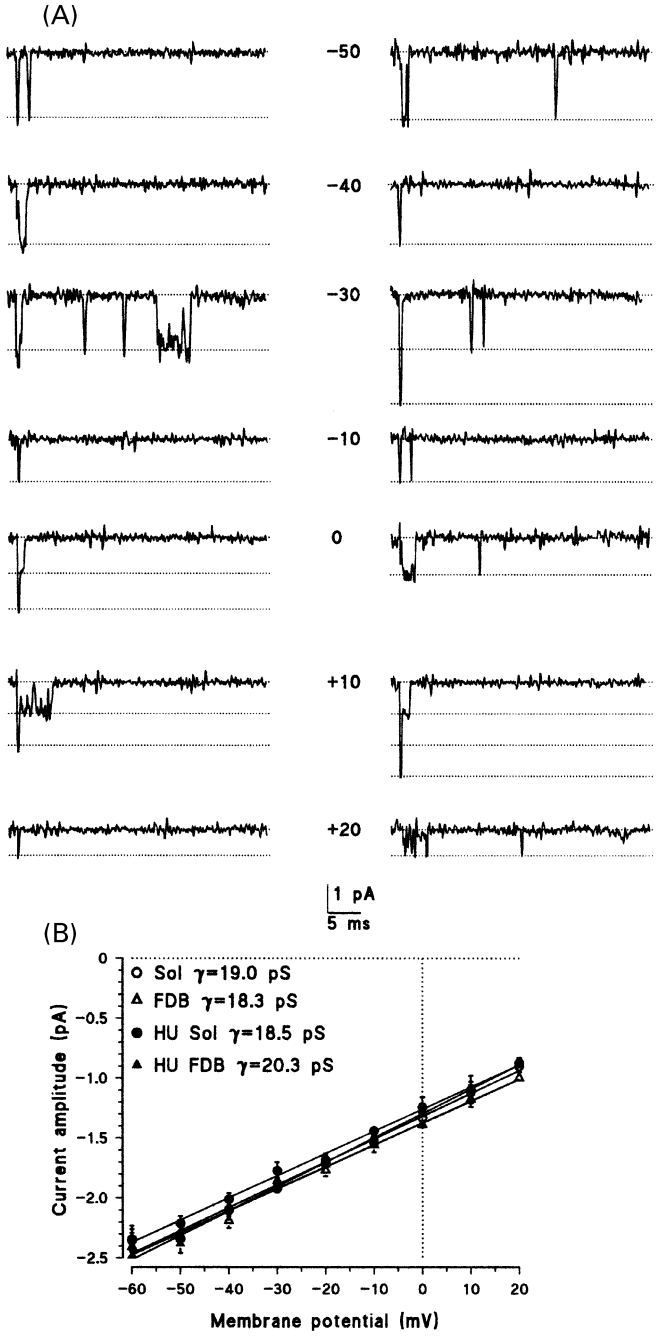

Fig. 2 Hindlimb unloading (HU) does not alter sodium channel unitary conductance. (**A**) Na^+ current traces from representative control (*left panel*) and 3-week HU (*right panel*) soleus muscle fibres are shown. The currents were elicited from a holding potential below –70 mV to reduce the number of overlapping channel openings. The test potentials are shown in mV. The dotted lines show the zero current level and open levels for one, two and three channels. (**B**) Single-channel current amplitudes plotted as a function of test potential for control and 3-week HU FDB and soleus (Sol) muscle fibres. Each shows the mean and standard error of the mean of current amplitude determined in at least three patches. The lines show the linear regression of data points, the slope of which gives a value of the unitary conductance, γ, as indicated in the figure.

Table 3 *Open probability of sodium channels at –20 mV in fast- and slow-twitch muscle fibres in control rats and rats that had been subjected to 3 weeks of hindlimb unloading (HU)*

	$P_{o,max}$	P_o
Control FDB (n = 9)	0.80 ± 0.02	0.46 ± 0.03
Control soleus (n = 7)	0.74 ± 0.02	0.37 ± 0.02*
HU FDB (n = 6)	0.82 ± 0.02	0.48 ± 0.02
HU soleus (n = 13)	0.76 ± 0.02	0.41 ± 0.02

The open probability of sodium channels was calculated for ensemble average currents constructed from at least 40 current records elicited by depolarizing the cell-attached patch membrane from –100 to –20 mV. The maximal open probability ($P_{o,max}$) and the total open probability (P_o) were calculated by dividing the peak amplitude and the time integral of ensemble average currents by the single-channel amplitude and the number of channels available. Data are mean ± standard error of the mean for n patches. *$P < 0.05$ versus the respective FDB muscle fibres (unpaired Student's t test).

currents elicited at –20 mV by the single-channel current, i, and the number of channels available, N (Table 3). The product iN was determined as the maximal peak current amplitude recorded within at least 100 consecutive depolarizing test pulses, assuming an open probability close to unity in this sweep (Kimitsuki *et al.*, 1990*a*). The open probability of sodium channels in cell-attached patches of FDB muscle fibres appeared about twofold greater than the value we had measured previously in inside-out patches (Desaphy *et al.*, 1998*b*, *c*). Such a difference was observed constantly between the two patch configurations and, even in the same patch, current amplitude greatly decreased when passing from the cell-attached to the inside-out patch configuration. Although never reported for sodium channels, similar behaviour has been described for other channels and is generally referred to as channel rundown (Becq, 1996). According to hypotheses formulated for other channels, it is possible that the patch excision to pass in inside-out configuration may disrupt interaction between the sodium channel protein and the cytoskeleton in a way that reduces open probability, or that the experimental solution bathing the intracellular side of the excised patch is not as favourable as the cytosol for the opening of sodium channels. The open probability of sodium channels in soleus muscle fibres generally appeared slightly lower than that measured in FDB muscle fibres of the same animals (Table 3). Hindlimb unloading did not have any effect on P_o and $P_{o,max}$ in either type of muscle. Therefore, the above results suggest, by exclusion, that the differences in sodium current amplitude at –20 mV between FDB and soleus muscle fibres of control rats and between control and HU soleus muscle fibres may be due mainly to differences in the number of channels available. To confirm this hypothesis it is necessary to

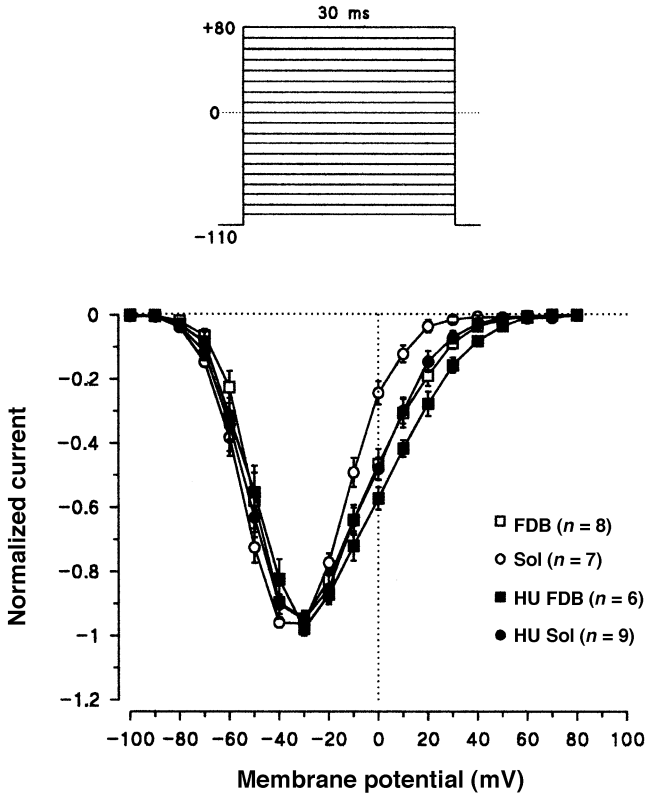

Fig. 3 Mean current–voltage relationships for sodium currents recorded in FDB and soleus (Sol) muscle fibres. Peak amplitudes were measured on macroscopic-current-like sodium currents elicited at test potentials ranging from –100 to +80 mV from a holding potential of –110 mV and normalized with respect to the maximal amplitude. Each data point shows the mean and standard error of the mean for *n* fibres for control and 3-week unloaded (HU), FDB and soleus muscles.

investigate the voltage-dependence of sodium currents in both type of muscles.

Effect of hindlimb unloading on the voltage-dependence of Na^+ channels

Sodium currents were observed between –80 and +60 mV and peaked between –40 and –20 mV, as reported previously (Desaphy *et al.*, 1998*a*). All normalized current–voltage (*I*/*V*) curves were closely superimposed, indicating the lack of difference in the voltage-dependence of sodium channel activation between FDB and soleus muscle fibres in both experimental conditions (Fig. 3). The voltage-dependence of the activation curves, constructed from the *I*/*V* curves by converting current to conductance (Desaphy *et al.*, 1998*a*), were very similar (not shown).

Sodium channels are known to undergo two distinct inactivation processes. The fast inactivation process has a time scale of a few milliseconds, whereas the slow inactivation process runs with a time constant of the order of seconds (Ruff *et al.*, 1987; Simoncini and Stühmer, 1987). Figure 4 shows that, in acutely dissociated skeletal muscle fibres, steady-state fast inactivation was already reached after a depolarizing voltage step of 50 ms. Prolonging the depolarizing period to 450 or 2000 ms did not modify the voltage-dependence of fast inactivation (Fig. 4D and E). Total fast inactivation was also quickly removed by a 50 ms hyperpolarizing step at –140 mV (Fig. 4F). Recent data indicate that slow and fast inactivation are not exclusive, i.e. a channel may be fast and slow inactivated simultaneously, but that the behaviour of the fast inactivation gate is independent of the state of the slow inactivation gate (Vedantham and Cannon, 1998). On this basis, slow inactivation occurring during a 2 s depolarizing voltage step can be unmasked if channels are allowed to recover from fast inactivation by a 50 ms hyperpolarizing step (Fig. 4G). In contrast to the fast inactivation curve, the slow inactivation curve did not reach zero current level, indicating that not all the channels entered slow inactivation. According to studies that addressed the time course of the development of slow inactivation, a 2 s conditioning voltage pulse may not be enough to reach the steady state of slow inactivation, especially at more negative potentials (Ruff, 1999; Hayward *et al.*, 1999; Struyk *et al.*, 2000). Unfortunately, using longer conditioning voltage pulses was particularly difficult in our experimental conditions owing to the limited lifetime duration of cell-attached patches, and we decided therefore to investigate slow inactivation at a time point different from the steady state.

On average, the half-maximum fast inactivation potential V_h of FDB muscle fibres of the control rats was –92.5 ± 1.6 mV (n = 8). It has been shown by us (Desaphy *et al.*, 1998*a*) and by others (Kimitsuki *et al.*, 1990*b*) that a negative shift in the voltage-dependence of sodium channel gating generally occurs during long-duration cell-attached patch recordings. Therefore, we always took care to perform inactivation voltage protocols at approximately the same time (between 20 and 30 min) to allow comparison between patches. In these conditions, we found no difference in the voltage-dependence of steady-state fast inactivation between FDB and soleus muscle fibres (Fig. 5A and Table 4). Furthermore, fast inactivation was not modified during 3 weeks of HU.

Sodium channel slow inactivation was also evaluated >20 min after gigaseal formation, even if no shift in slow inactivation voltage-dependence was reported during long patch recordings (O'Reilly *et al.*, 1999). As described above, fast-inactivated sodium channels were allowed to recover at –140 mV for 50 ms to reveal sodium channels that had entered the slow inactivated state during a 2 s depolarization. In these conditions, no difference was observed in slow inactivation voltage-dependence between fast- and slow-twitch muscle fibres (Fig. 5B and Table 4). After 3 weeks of HU, we observed only a small, non-significant reduction in the proportion of slow inactivated channels in both muscle types (Fig. 5B and Table 4).

As the voltage-dependence of sodium channels was not

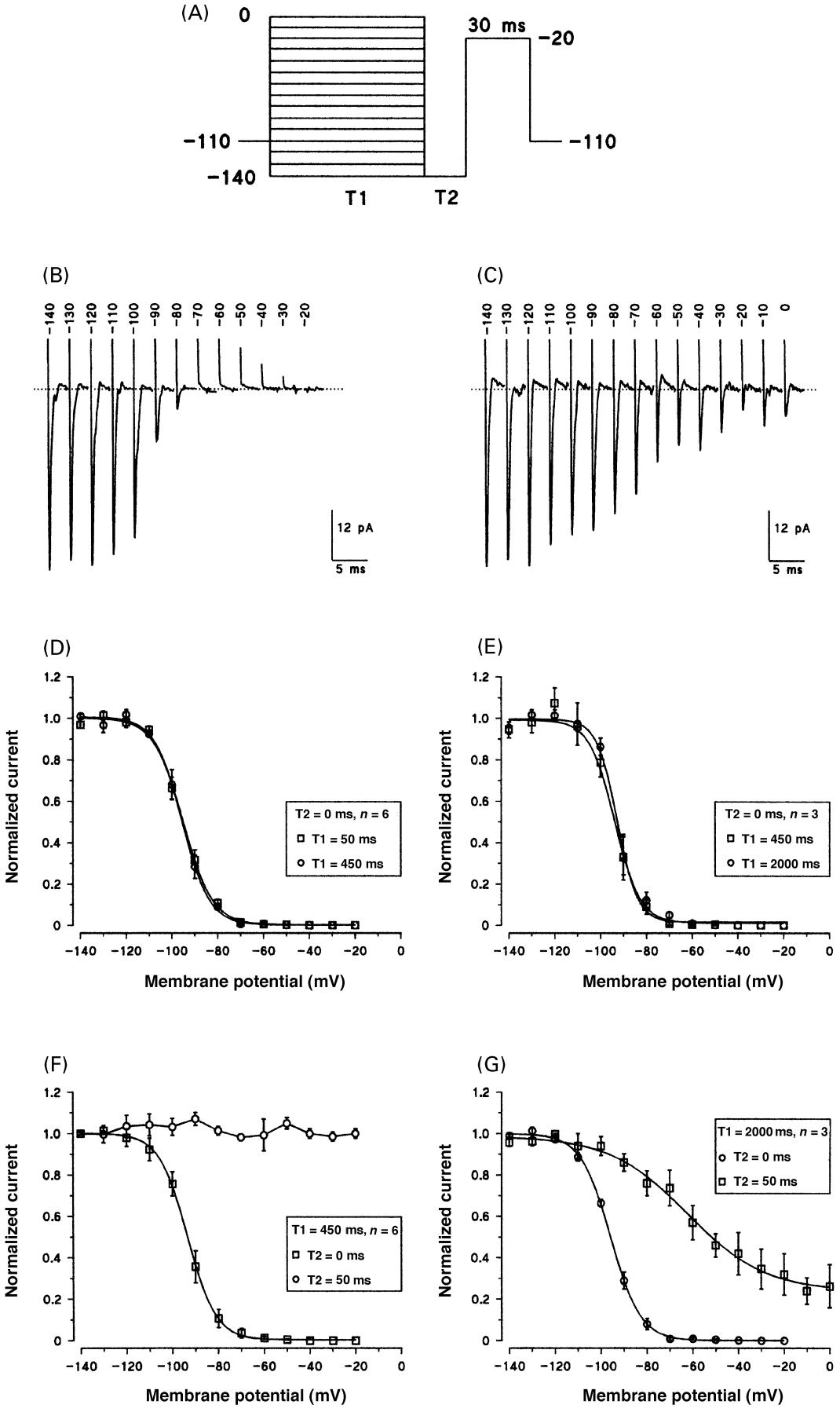
(A)
0
30 ms
-20
-110
-110
-140
T1
T2
(B)
-140 -130 -120 -110 -100 -90 -80 -70 -60 -50 -40 -30 -20
12 pA
5 ms
(C)
-140 -130 -120 -110 -100 -90 -80 -70 -60 -50 -40 -30 -20 -10 0
12 pA
5 ms
(D)
Normalized current
T2 = 0 ms, n = 6
T1 = 50 ms
T1 = 450 ms
Membrane potential (mV)
(E)
Normalized current
T2 = 0 ms, n = 3
T1 = 450 ms
T1 = 2000 ms
Membrane potential (mV)
(F)
Normalized current
T1 = 450 ms, n = 6
T2 = 0 ms
T2 = 50 ms
Membrane potential (mV)
(G)
Normalized current
T1 = 2000 ms, n = 3
T2 = 0 ms
T2 = 50 ms
Membrane potential (mV)

Table 4 *Steady-state inactivation parameters of sodium channels in fast and slow twitch muscle fibres in control rats and rats that had been subjected to 3 weeks of hindlimb unloading (HU)*

	Fast inactivation			Slow inactivation		
	V_h (mV)	K_h (mV)	I_{max} (–pA)	V_s (mV)	K_s (mV)	I_{min}/I_{max}
Control FDB	–92.5 ± 1.6 (n = 8)	5.8 ± 0.4 (n = 7)	116.8 ± 16.4	–64.2 ± 2.0	14.3 ± 0.6	0.19 ± 0.05
Control soleus	–94.6 ± 0.1 (n = 7)	5.0 ± 0.4 (n = 7)	20.0 ± 2.8*	–66.9 ± 2.1	13.9 ± 1.2	0.22 ± 0.03
HU FDB	–94.6 ± 2.8 (n = 6)	5.7 ± 0.2 (n = 4)	79.8 ± 6.9	–61.4 ± 3.0	14.0 ± 1.3	0.27 ± 0.09
HU soleus	–94.2 ± 1.5 (n = 9)	5.9 ± 0.2 (n = 7)	73.7 ± 20.2**	–63.7 ± 2.9	15.8 ± 1.4	0.27 ± 0.03

All parameters are derived from the fit with the Boltzmann equation of non-normalized steady-state fast and slow inactivation curves obtained in individual patches and are expressed as mean ± standard error of the mean. V_h = half-maximal fast inactivation potential; K_h = fast-inactivation slope factor; I_{max} = maximal sodium current; V_s = half-maximal slow inactivation potential; K_s = slow inactivation slope factor; I_{min}/I_{max} = minimal/maximal current ratio. *$P < 0.001$ versus control FDB; **$P < 0.05$ versus control soleus (unpaired Student's t test).

different between control soleus and FDB muscles or between control and 3-week HU muscles, the differences observed in sodium current amplitude at –20 mV resulted from differences in the density of sodium channels present in the patch.

Effect of hindlimb unloading on Na^+ channel expression in soleus muscle

To calculate sodium channel density as a measure of sodium channel protein expression, the maximal sodium current I_{max}, measured on non-normalized steady-state inactivation curves, was divided by the square of the pipette conductance. After 1 week of HU, sodium current density was already significantly higher than in control soleus muscles and regularly increased during the HU period from 1 to 3 weeks (Fig. 6A). In adult skeletal muscles, sodium channels are heterodimers consisting of one α subunit, which forms the ion-conducting pore with intrinsic voltage- and time-dependent properties, and one auxiliary β_1 subunit, which modulates channel insertion in the membrane and channel-gating properties (for review, see Marban *et al.*, 1998). The adult skeletal muscle α subunit isoform, SkM1, is encoded by the *SCN4A* gene (Trimmer *et al.*, 1989), whereas the ubiquitous β_1 subunit is encoded by the gene *SCN1B* (Makita *et al.*, 1994). We determined the gene transcript levels for both subunits in control soleus muscles and in soleus muscles after 1 or 3 weeks of HU. The level of SkM1 mRNA was found to increase twofold after 1 week of HU but, surprisingly, recovered to the control level after 3 weeks of HU (Fig. 6B). In contrast, the mRNA level for the β_1 subunit remained unchanged after 1 week of HU but increased after 3 weeks of HU (Fig. 6C).

Absence of denervation in 3-week unloaded soleus muscles

Adult skeletal muscle fibres express almost exclusively the skeletal muscle-specific sodium channel isoform SkM1. However, after denervation, an increase in total sodium-channel mRNA synthesis has been reported together with the appearance of the juvenile sodium channel isoform SkM2, the same channel as that expressed in the heart, which is resistant to tetrodotoxin (Kallen *et al.*, 1990; Yang *et al.*, 1991). To exclude denervation from our model, we tested the sensitivity to tetrodotoxin of sodium channels expressed in soleus muscle fibres of 3-week HU rats by performing

Fig. 4 Characterization of fast and slow inactivation voltage-dependence of sodium currents in cell-attached macropatches of skeletal muscle fibres. (**A**) General voltage protocol to measure fast and slow inactivation voltage-dependence. The times T1 and T2 are given for each curve shown in **D**, **E**, **F** and **G**. (**B** and **C**) Current samples were recorded during the 30 ms test pulse at –20 mV in a soleus muscle fibre of a control rat using T1 = 2000 ms and T2 = 0 ms (**B**) or T2 = 50 ms (**C**). The conditioning potential held during T1 is indicated above each current trace. The results obtained from this fibre are included in the curves of panel **G**. (**D**–**G**) The protocol was repeated five times in each patch; peak sodium current amplitudes were measured during the 30 ms test pulse at –20 mV and were averaged to obtained reliable values. These values were plotted as a function of the potential held for time T1 and fitted with the Boltzmann equations described in the Material and methods section. Values were then normalized with respect to the maximal amplitude (I_{max}) obtained from the fit and finally averaged from n fibres to obtain the mean and standard error of the mean. One exception is for the relationship shown in **D** with T2 = 50 ms; this relationship was not fitted and current amplitudes were normalized with respect to that obtained at –140 mV before being averaged from n fibres. The normalized relationships obtained from n cells were fitted with the Boltzmann equation. Each graph compares two curves obtained in the same n fibres by varying T1 or T2 in the protocol. The fibres were from 3-week unloaded soleus muscles (**D**), 3-week unloaded FDB muscles (**E**), control FDB muscles (**F**) and control soleus muscles (**G**).

three consecutive patches on each fibre with patch pipettes of similar diameters, as described previously (Desaphy *et al.*, 1998*b*). The first and third patches were performed as control and recovery, respectively, whereas the second patch was performed with 100 nM tetrodotoxin in the pipette solution (Fig. 7A). In the presence of tetrodotoxin, the peak amplitude of sodium current, elicited from –100 to –20 mV, was 8.0 ± 1.9% of the control peak current (–7.0 ± 2.0 and –87.3 ± 5.2 pA, respectively; $n = 4$, $P < 0.001$). The reduction in current amplitude in the second patch was not due to run-down because currents elicited in the third patch were similar to control currents (–75.7 ± 1.3 and –83.6 ± 4.5 pA, respectively; $n = 3$, $P > 0.1$). For comparison, while 100 nM tetrodotoxin blocked ~95% of the sodium current of innervated FDB and extensor digitorum longus muscle fibres of normal rats (Pappone, 1980; Desaphy *et al.*, 1998*b*), up to 35% of the sodium current remained unaffected by the toxin in denervated muscle fibres (Pappone, 1980). We also looked at the expression of SkM2 mRNA in HU soleus muscles and, to verify the specificity of our probe, in a soleus muscle and the heart of one control rat (Fig. 7B). No SkM2 transcript was detected in soleus muscles of four 3-week HU rats. Therefore, there was no sign of a denervation process in soleus muscles subjected to this ground-model of microgravity.

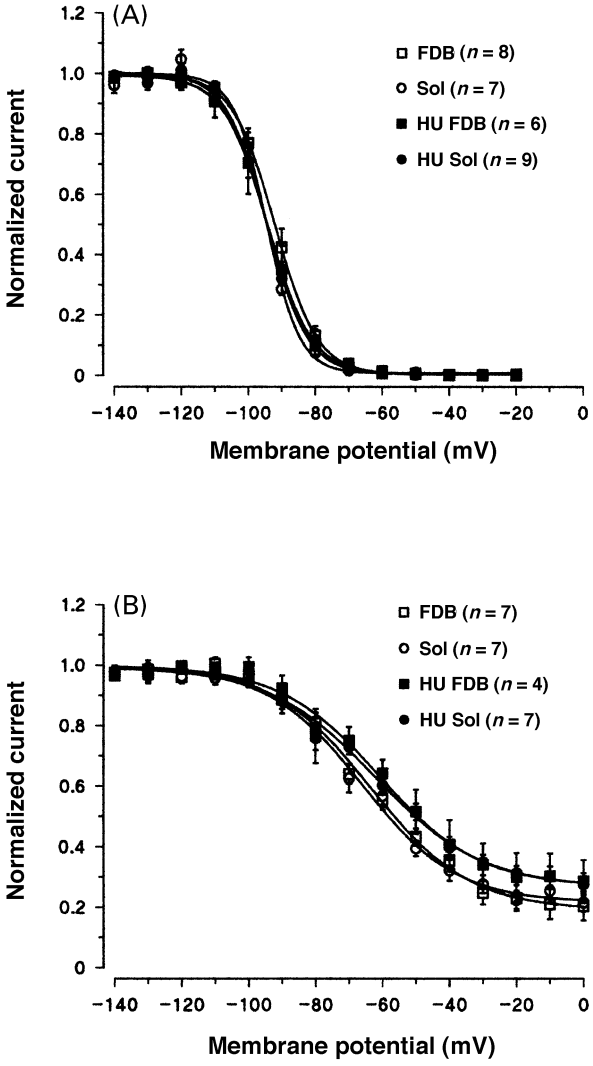

Fig. 5 Effect of hindlimb unloading (HU) on fast and slow inactivation voltage-dependence of sodium currents recorded in FDB and soleus (Sol) muscle fibres. (**A**) Fast steady-state inactivation relationships were obtained using the voltage protocol described in Fig. 4 with T1 = 50 ms and T2 = 0 ms. The parameters of the Boltzmann fits obtained from the non-normalized relationships are given in Table 4. Current amplitudes were then normalized by I_{max} to allow direct comparison of steady-state inactivation curves obtained from n fibres of control and 3-week HU FDB and soleus muscles. (**B**) Slow inactivation relationships were obtained from the voltage protocol described in Fig. 4 with T1 = 2000 ms and T2 = 50 ms. The parameters of the Boltzmann fits obtained from the non-normalized relationships are given in Table 4. Current amplitudes were then normalized by I_{max} to allow direct comparison of the curves obtained from n fibres of control and 3-week HU FDB and soleus muscles.

Discussion

Sodium channel differences between slow- and fast-twitch muscle fibres

The diversification of slow-twitch and fast-twitch muscles occurs naturally during development, under the control of motor neurone electrical activity (Buonanno and Fields, 1999) but also in relation to muscle cell lineage (Hughes and Salinas, 1999). Thus, skeletal muscle fibres acquire specific contractile properties that permit them to respond to specific needs. Muscle specificity resides in a number of gene products involved in contractility, calcium handling, metabolism and, although less studied, sarcolemma excitability. Sodium channel distribution has been reported to differ between slow- and fast-twitch muscles of mice, rats and humans (Milton *et al.*, 1992; Ruff, 1992; Ruff and Whittlesey, 1993*a*; Milton and Behforouz, 1995). Using the loose-patch voltage-clamp technique, these authors showed that both the end-plates and the extrajunctional sarcolemma of fast-twitch muscle fibres exhibit a higher (between two- and sixfold) sodium current density than that of slow-twitch muscles. When we applied the cell-attached patch-clamp technique to extrajunctional sarcolemma, we obtained a similar result with FDB muscle fibres, which exhibited a sodium current density about five times greater than that of soleus muscle fibres. By increasing muscle excitability, a higher sodium current density may allow the higher mechanical threshold observed in fast-twitch fibres to be counteracted to some extent, because a faster rising phase of the action potential in fast-twitch muscle fibres means that the mechanical threshold, though higher than in slow-twitch muscle fibres, would be reached sooner (Dulhunty, 1980). Furthermore, increased sodium current density on or near the end-plates of fast-twitch muscle fibres may increase the safety factor for neuromuscular transmission in these fibres (Ruff, 1992; Wood and Slater, 1995; Ruff and Lennon, 1998). Alternatively, the reduced entry of Na^+ ions, together with the higher Na^+, K^+ ATPase activity in

slow-twitch muscle fibres, would limit the accumulation of K^+ ions in the extracellular space and consequently may increase resistance to fatigue, allowing these fibres to be tonically active (Harrison *et al.*, 1997).

Phenotypic differences have also been reported in the voltage dependencies of the fast and slow inactivation processes of sodium channels using the double sucrose-gap technique (Duval and Léoty, 1978, 1980) and the loose patch-clamp technique (Ruff *et al.*, 1987; Ruff and Whittlesey, 1993*a*). These authors reported that sodium channels inactivate at potentials less negative in slow- than in fast-twitch muscle fibres, suggesting that slow-twitch fibres are relatively resistant to the fatigue associated with reduced membrane excitability because they are resistant to channel inactivation. Using the cell-attached patch-clamp technique, we found no evidence of such differences in sodium channel gating properties between the two fibre types. The discrepancy with respect to earlier voltage-clamp experiments may result from differences in the electrophysiological techniques or the method of preparation of native fibres. On the other hand, the similarities we found in sodium channel permeation and gating properties between slow- and fast-twitch muscle fibres strongly support the idea that the two fibre types express the same channel protein. Another inconsistency in the literature concerns the voltage-dependence of slow inactivation. Whereas the value of V_s we determined in the present study (~–65 mV) is in agreement with that reported by some others (e.g. Cummins and Sigworth, 1996; Hayward *et al.*, 1997; O'Reilly *et al.*, 1999; Struyk *et al.*, 2000), other workers have found a less negative (Bielefeldt *et al.*, 1999) or more negative V_s (Simoncini and Stühmer, 1987; Ruben *et al.*, 1992; Ruff and Whittlesey, 1993*b*; Townsend and Horn, 1997; Ruff, 1999). There is also a discrepancy in the completeness of slow inactivation, which may eliminate Na^+ currents totally (Ruff and Whittlesey, 1993*a*; 1993*b*; Ruff, 1999) or may leave 5–25% of channels active (Cummins and Sigworth, 1996; Hayward *et al.*, 1997; Bielefeldt *et al.*, 1999; O'Reilly *et al.*, 1999; Struyk *et al.*, 2000). These issues have been addressed and discussed extensively in several

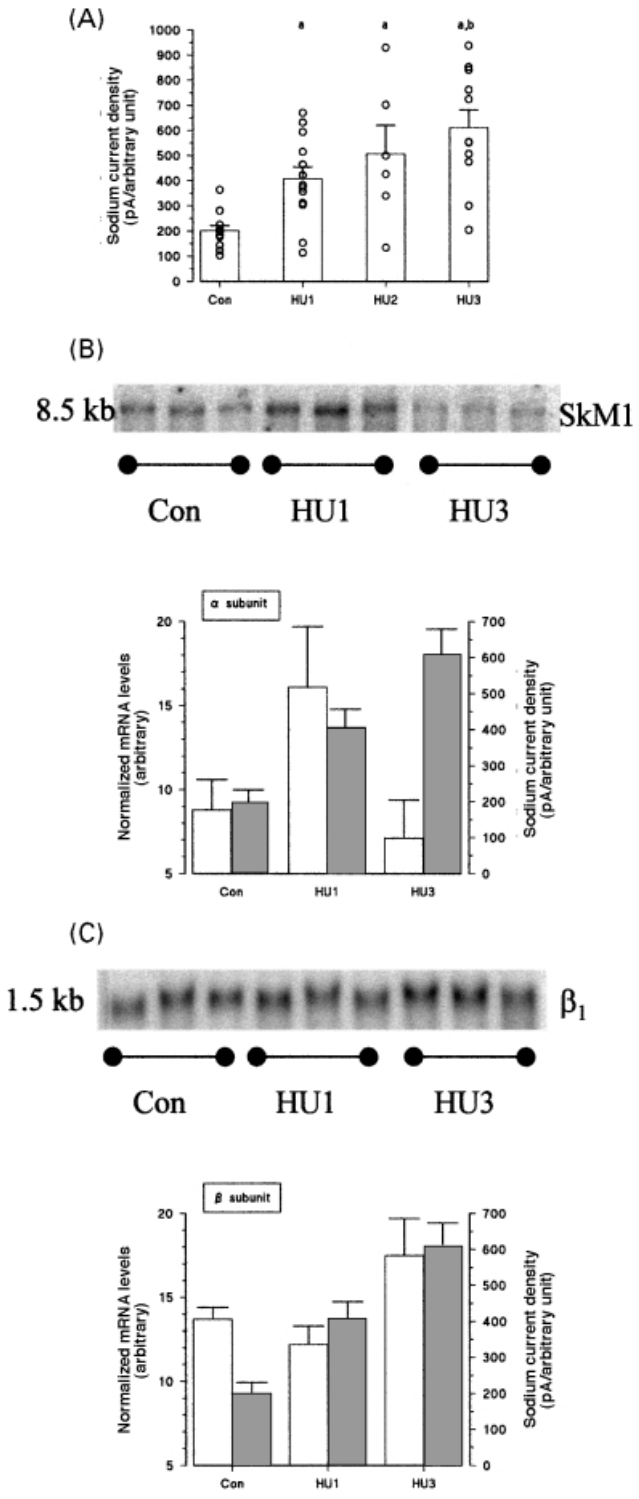

Fig. 6 Sodium channel expression in soleus muscle. (**A**) Sodium current density was calculated by dividing the maximal current measured on steady-state inactivation curves by the square of the pipette conductance. Circles show individual values measured in soleus muscle fibres of control rats (Con) and rats suspended for 1 (HU1), 2 (HU2) or 3 (HU3) weeks. Bars represent the mean and standard error of the mean for individual values. $^aP < 0.05$ or less versus control; $^bP < 0.05$ or less versus 1-week HU (unpaired Student's t test). (**B**) Northern blot analysis of soleus muscles of control rats and rats suspended for 1 or 3 weeks using a specific probe for the α subunit of the skeletal muscle sodium channel SkM1. Each line represents a single soleus muscle. The histogram shows SkM1 mRNA levels normalized with respect to the 18 S ribosomal RNA. Each open bar represents the mean and standard error of the mean for soleus muscles isolated from at least six animals. Use of the unpaired Student's t test gave $P < 0.1$ for 1-week HU versus control and 3-week HU. The shaded bars show the progression of sodium current density. (**C**) Northern blot analysis of soleus muscles of control rats and rats suspended for 1 or 3 weeks using a specific probe for the β_1 subunit of sodium channels. Each line represents a single soleus muscle. The histogram shows β_1 mRNA levels normalized with respect to the 18 S ribosomal RNA. Each bar represents the mean and standard error of the mean for soleus muscles isolated from at least six animals. Use of the unpaired Student's t test gave $P < 0.1$ between 3-week HU and control and $P < 0.05$ between 3- and 1-week HU.

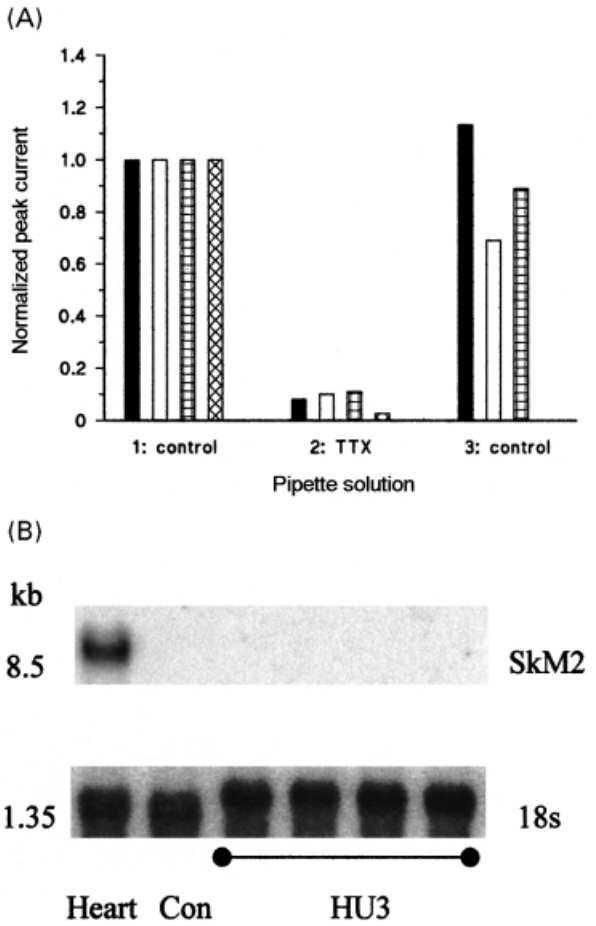

Fig. 7 Absence of expression of the tetrodotoxin (TTX)-resistant sodium channel SkM2 in soleus muscles after hindlimb unloading (HU). (**A**) Sensitivity of sodium currents to 100 nM tetrodotoxin in soleus muscle fibres isolated from four rats suspended for 3 weeks. Two or three cell-attached patches were performed on a small delimited area of the same fibre with (second patch) or without (first and third patches) 100 nM tetrodotoxin in the pipette. The pipettes used on each fibre were chosen to have the same diameter. Each bar-filling pattern corresponds to one fibre. Each bar represents the peak amplitude of ensemble average currents elicited in each patch by depolarizing the membrane from –100 to –20 mV and normalized with respect to that found in the first patch. (**B**) Northern blot analyses of one heart and one soleus muscle isolated from a control rat (con) and of soleus muscles isolated from 3-week HU rats (HU3), using a specific probe for the α subunit of the cardiac sodium channel SkM2 and an 18 S ribosomal RNA probe as control. Each line represents a single soleus muscle.

studies (e.g. Cummins and Sigworth, 1996; Ruff, 1999; see comments in Hayward *et al.*, 1999), but no clear explanation has emerged. It should be kept in mind that slow inactivation may include multiple time-dependent states ranging from intermediate (Kambouris *et al.*, 1998) to ultra-slow (Furue *et al.*, 1998; Todt *et al.*, 1999) components rather than a unique process. Moreover, slow inactivation appeared to be sensitive to various modulations, including temperature (Ruff, 1999), ionic strength (Townsend and Horn, 1997), β_1 subunit expression (Vilin *et al.*, 1999) and nitric oxide-dependent nitrosylation (Bielefeldt *et al.*, 1999). All these features might help resolve to these controversies.

Effect of muscle unloading on sodium channel expression

Disuse of human and rodent slow-twitch muscles, as provoked by exposure to microgravity during space flight, muscle immobilization and hind limb suspension, has been shown to induce muscle atrophy and to modify the expression of a number of proteins in a way that mostly corroborates the well-documented switch of muscle phenotype from slow to fast (Talmadge, 2000). The present results add sodium channels to the list of proteins. After 1 week of muscle unloading, sodium current density in extrajunctional sarcolemma of soleus muscle fibres has undergone a twofold increase and after 3 weeks of unloading it reaches a level ~65% of that measured in FDB muscle fibres. In adult skeletal muscle, sodium currents are carried by the muscle-specific, tetrodotoxin-sensitive sodium channel α subunit, SkM1 (Trimmer *et al.*, 1989), associated with the ubiquitous β_1 subunit (Makita *et al.*, 1994). Skeletal muscle is also known to express the cardiac isoform of the tetrodotoxin-resistant sodium channel α subunit, called H1 or SkM2, during development or after denervation (Kallen *et al.*, 1990; Yang *et al.*, 1991). However, in HU soleus muscle fibres, sodium currents were highly sensitive to tetrodotoxin and no trace of transcript of the gene encoding SkM2 was found, thus excluding *de novo* expression of this channel. Similarities in gating and permeation properties as well as in the tetrodotoxin sensitivity of sodium currents in soleus muscle fibres before and after suspension strongly argue for increased expression of SkM1 channels in HU slow-twitch muscle fibres. This was confirmed at 1 week of muscle unloading by the 2-fold increase in the level of mRNA for the SkM1 α subunit, which was strictly parallel to the 2-fold increase in sodium current density. Yet such a correlation was not observed after 3 weeks of HU, when the mRNA level for SkM1 had returned towards the control level whereas the sodium current density was still increasing. Although we cannot completely exclude the expression of another tetrodotoxin-sensitive sodium channel α subunit, such as the brain type II, the increased channel density in the sarcolemma after 3 weeks of muscle unloading may have been due to a change in SkM1 protein turnover resulting from the increased expression of the β_1 subunit, which has been shown to promote channel incorporation in membranes (Isom *et al.*, 1992).

The mechanisms underlying the increased transcription of the *SCN4A* and *SCN1B* genes remain unknown. Nevertheless, it has been shown recently that the promoter region of *SCN4A* contains two E boxes, one of which plays a critical role in tissue-specific gene expression under the positive control of members of the MyoD family of transcription factors (Kraner *et al.*, 1998). As hindlimb suspension has been shown to

activate the expression of MyoD in soleus muscle fibres (Wheeler *et al.*, 1999), this factor is a good candidate for the upregulation of SkM1 expression. Nevertheless, other factors may act synergistically with MyoD (Kraner *et al.*, 1999), and are perhaps related to cytosolic calcium and cyclic AMP, which regulates the level of SkM1 α subunit mRNA in an interdependent manner (Offord and Catterall, 1989). Interestingly, the resting cytosolic calcium may be augmented in the soleus muscle after HU (Ingalls *et al.*, 1999), although other results suggest that calcium may trigger the opposite, fast-to-slow transition of muscle phenotype, most probably through activation of the cyclosporin-sensitive calcineurin–NFAT (nuclear factor of activated t cells) pathway (Chin *et al.*, 1998; Meissner *et al.*, 2000). Transcription factors may be activated by the changes in electrical activity and concentrations of hormones (e.g. thyroid hormone) that occur during muscle disuse (Blewett and Elder, 1993; Stein *et al.*, 1999) and which are known to modulate sodium channel expression (Brodie and Sampson, 1989; Offord and Catterall, 1989; Chahine *et al.*, 1993). Importantly, the intracellular machinery turned on by HU should be different from that involved in the response to denervation, as the latter is known to induce *de novo* expression of SkM2 channels whereas little change in SkM1 transcript level is observed (Yang *et al.*, 1991). Whereas some transcription factors can be affected similarly by denervation and HU (e.g. the MyoD level increases in both situations), some others are probably regulated differently in order to obtain a specific response (e.g. the myogenin level increases after denervation but remains constant after HU) (Klocke *et al.*, 1994; Wheeler *et al.*, 1999). Such features underline the complexity of gene control by external signals and indicate that the effect of HU is to modify the use of slow muscles rather than render them inactive. The return to control levels of α subunit mRNA after 3 weeks of HU is very surprising, but might constitute an adaptation of the slow-twitch muscles to long-term disuse, together with the delayed increase in the β_1 subunit transcript. Parallelism between SkM1 α subunit and β_1 subunit expression has been shown during postnatal development, after surgical denervation and in primary muscle cell culture (Yang *et al.*, 1993). Nevertheless, our data suggest that the *SCN4A* and *SCN1B* genes may be regulated independently in skeletal muscle, at least in certain conditions. In support of this, independent regulation of α and β_1 subunits has been reported in other tissues, such as the foetal brain (Patton *et al.*, 1994) and the denervated olfactory system (Sashihara *et al.*, 1996). More recently, protein kinase C-dependent opposite regulation of α and β_1 subunit mRNA levels has also been reported in adrenal chromaffin cells (Yanagita *et al.*, 1999).

Pathophysiological relevance of increased Na^+ channel density in slow-twitch muscle fibres

Sodium channels are pivotal for the genesis of action potentials in excitable cells. In neurones, action potentials have been shown to regulate gene expression (Fields *et al.*, 1997) and the modulation of sodium-channel expression is considered to be a basis for functional plasticity (Waxman, 2000). In skeletal muscle, a high density of sodium channels in the sarcolemma allows fast-twitch fibres to fire at high frequencies in order to allow rapid and potent contraction, whereas slow-twitch muscle fibres do not require channel density to be so high in order to respond to slow motor neurone input. Moreover, a lower sodium channel density in slow-twitch muscle fibres may reduce the propensity to fatigue during long periods of tonic activity. Veratridine and aconitine, activators of sodium channels, have been shown to decrease muscle endurance greatly and to slow the initial rate of force recovery in rat soleus muscle (Harrison *et al.*, 1997). This effect has been attributed to an increase in sodium influx exceeding the capacity of Na^+,K^+ ATPase to remove Na^+ from the sarcoplasma. Similarly, if not compensated for by a simultaneous increase in Na^+,K^+ pump activity, the increase in sodium current density in the extrajunctional sarcolemma that we observed in response to hindlimb suspension may greatly influence the characteristics of contraction and in particular may reduce the resistance to fatigue of antigravity muscle fibres. This probably contributes to the difficulty in maintaining posture and the reduction in motor capacity that humans undergo after space flight or a long period of immobilization. Finally, because a number of drugs are known to target sodium channels, the pharmacological block of these channels in slow-twitch muscles might represent a good therapeutic approach to counteracting disuse-induced muscle impairment.

Acknowledgements

This work was supported by a grant from the Italian Space Agency to D.C.C. (ASI ARS-99-33, ASI ARS-98-71 and ASI ARS-2000). J.-F.D. is a postdoctoral fellow of Telethon Italy.

References

Becq F. Ionic channel rundown in excised membrane patches. [Review]. Biochim Biophys Acta 1996; 1286: 53–63.

Bielefeldt K, Whiteis CA, Chapleau MW, Abboud FM. Nitric oxide enhances slow inactivation of voltage-dependent sodium currents in rat nodose neurons. Neurosci Lett 1999; 271: 159–62.

Blewett C, Elder GC. Quantitative EMG analysis in soleus and plantaris during hindlimb suspension and recovery. J Appl Physiol 1993; 74: 2057–66.

Brodie C, Sampson SR. Characterization of thyroid hormone effects on Na channel synthesis in cultured skeletal myotubes: role of Ca^{2+}. Endocrinology 1989; 125: 842–9.

Buonanno A, Fields RD. Gene regulation by patterned electrical activity during neural and skeletal muscle development. [Review]. Curr Opin Neurobiol 1999; 9: 110–20.

Chahine KG, Baracchini E, Goldman D. Coupling muscle electrical activity to gene expression via a cAMP-dependent second messenger system. J Biol Chem 1993; 268: 2893–8.

Chin ER, Olson EN, Richardson JA, Yang Q, Humphries C, Shelton JM, et al. A calcineurin-dependent transcriptional pathway controls skeletal muscle fiber type. Genes Dev 1998; 12: 2499–509.

Chomczynski P, Sacchi N. Single-step method of RNA isolation by acid guanidinium thiocyanate–phenol–chloroform extraction. Anal Biochem 1987; 162: 156–9.

Cummins TR, Sigworth FJ. Impaired slow inactivation in mutant sodium channels. Biophys J 1996; 71: 227–36.

Desaphy J-F, De Luca A, Camerino DC. Blockade by cAMP of native sodium channels of adult rat skeletal muscle fibers. Am J Physiol 1998a; 275: C1465–72.

Desaphy J-F, De Luca A, Imbrici P, Conte Camerino D. Modification by ageing of the tetrodotoxin-sensitive sodium channels in rat skeletal muscle fibres. Biochim Biophys Acta 1998b; 1373: 37–46.

Desaphy J-F, De Luca A, Pierno S, Imbrici P, Camerino DC. Partial recovery of skeletal muscle sodium channel properties in aged rats chronically treated with growth hormone or the GH-secretagogue hexarelin. J Pharmacol Exp Ther 1998c; 286: 903–12.

Dulhunty AF. Potassium contractures and mechanical activation in mammalian skeletal muscles. J Membr Biol 1980; 57: 223–33.

Duval A, Léoty C. Ionic currents in mammalian fast skeletal muscle. J Physiol (Lond) 1978; 278: 403–23.

Duval A, Léoty C. Ionic currents in slow twitch skeletal muscle in the rat. J Physiol (Lond) 1980; 307: 23–41.

Fields RG, Eshete F, Stevens B, Itoh K. Action potential-dependent regulation of gene expression: temporal specificity in Ca^{2+}, cAMP-responsive element binding proteins, and mitogen-activated protein kinase signaling. J Neurosci 1997; 17: 7252–66.

Furue T, Yakehiro M, Yamaoka K, Sumii K, Seyama I. Characteristics of two slow inactivation mechanisms and their influence on the sodium channel activity of frog ventricular myocytes. Pflügers Arch 1998; 436: 631–8.

Hamill OP, Marty A, Neher E, Sakmann B, Sigworth FJ. Improved patch-clamp techniques for high-resolution current recording from cells and cell-free membrane patches. Pflügers Arch 1981; 391: 85–100.

Harrison AP, Nielsen OB, Clausen T. Role of Na^+-K^+ pump and Na^+ channel concentrations in the contractility of rat soleus muscle. Am J Physiol 1997; 272: R1402–8.

Hayward LJ, Brown RH Jr, Cannon SC. Slow inactivation differs among mutant Na channels associated with myotonia and periodic paralysis. Biophys J 1997; 72: 1204–19.

Hayward LJ, Sandoval GM, Cannon SC. Defective slow inactivation of sodium channels contributes to familial periodic paralysis. Neurology 1999; 52: 1447–53.

Hughes SM, Salinas PC. Control of muscle fibre and motoneuron diversification. [Review]. Curr Opin Neurobiol 1999; 9: 54–64.

Ingalls CP, Warren GL, Armstrong RB. Intracellular Ca^{2+} transients in mouse soleus muscle after hindlimb unloading and reloading. J Appl Physiol 1999; 87: 386–90.

Isom LL, De Jongh KS, Patton DE, Reber BF, Offord J, Charbonneau H, et al. Primary structure and functional expression of the β_1 subunit of the rat brain sodium channel. Science 1992; 256: 839–42.

Kallen RG, Sheng Z-H, Yang J, Chen LQ, Rogart RB, Barchi RL. Primary structure and expression of a sodium channel characteristic of denervated and immature rat skeletal muscle. Neuron 1990; 4: 233–42.

Kambouris NG, Hastings LA, Stepanovic S, Marban E, Tomaselli GF, Balser JR. Mechanistic link between lidocaine block and inactivation probed by outer pore mutations in the rat μ1 skeletal muscle sodium channel. J Physiol (Lond) 1998; 512: 693–705.

Kazen-Gillespie KA, Ragsdale DS, D'Andrea MR, Mattei LN, Rogers KE, Isom LL. Cloning, localization, and functional expression of sodium channel β_1A subunits. J Biol Chem 2000; 275: 1079–88.

Kimitsuki T, Mitsuiye T, Noma A. Maximum open probability of single Na^+ channels during depolarization in guinea-pig cardiac cells. Pflügers Arch 1990a; 416: 493–500.

Kimitsuki T, Mitsuiye T, Noma A. Negative shift of cardiac Na^+ channel kinetics in cell-attached patch recordings. Am J Physiol 1990b; 258: H247–54.

Klocke R, Steinmeyer K, Jentsch TJ, Jockusch H. Role of innervation, excitability, and myogenic factors in the expression of the muscular chloride channel ClC-1. J Biol Chem 1994; 269: 27635–9.

Kraner SD, Rich MM, Kallen RG, Barchi RL. Two E-boxes are the focal point of muscle-specific skeletal muscle type 1 Na^+ channel gene expression. J Biol Chem 1998; 273: 11327–34.

Kraner SD, Rich MM, Sholl MA, Zhou H, Zorc CS, Kallen RG, et al. Interaction between the skeletal muscle type 1 Na^+ channel promoter E-box and an upstream repressor element. J Biol Chem 1999; 274: 8129–36.

Makita N, Bennett PB Jr, George AL Jr. Voltage-gated Na^+ channel β_1 subunit mRNA expressed in adult human skeletal muscle, heart, and brain is encoded by a single gene. J Biol Chem 1994; 269: 7571–8.

Marban E, Yamagaishi T, Tomaselli GF. Structure and function of voltage-gated sodium channels. [Review]. J Physiol (Lond) 1998; 508: 647–57.

Meissner JD, Kubis H-P, Scheibe RJ, Gros G. Reversible Ca^{2+}-induced fast-to-slow transition in primary skeletal muscle culture cell at the mRNA level. J Physiol (Lond) 2000; 523: 19–28.

Milton RL, Behforouz MA. Na channel density in extrajunctional sarcolemma of fast and slow twitch mouse skeletal muscle fibres: functional implications and plasticity after fast motoneuron transplantation on to a slow muscle. J Muscle Res Cell Motil 1995; 16: 430–9.

Milton RL, Lupa MT, Caldwell JH. Fast and slow twitch skeletal muscle fibres differ in their distribution of Na channels near the endplate. Neurosci Lett 1992; 135: 41–4.

Morey ER. Space flight and bone turnover: correlation with a new rat model of weightlessness. Bioscience 1979; 29: 168–72.

Offord J, Catterall WA. Electrical activity, cAMP, and cytosolic calcium regulate mRNA encoding sodium channel α subunits in rat muscle cells. Neuron 1989; 2: 1447–52.

O'Reilly JP, Wang S-Y, Kallen RG, Wang GK. Comparison of slow inactivation in human heart and rat skeletal muscle Na^+ channel chimaeras. J Physiol (Lond) 1999; 515: 61–73.

Pappone PA. Voltage-clamp experiments in normal and denervated mammalian skeletal muscle fibres. J Physiol (Lond) 1980; 306: 377–410.

Patton DE, Isom LL, Catterall WA, Goldin AL. The adult rat brain beta1 subunit modifies activation and inactivation gating of multiple sodium channel alpha subunits. J Biol Chem 1994; 269: 17649–55.

Pette D, Vrbovà G. Adaptation of mammalian skeletal muscle fibers to chronic electrical stimulation. [Review]. Rev Physiol Biochem Pharmacol 1992; 120: 115–202.

Pierno S, De Luca A, Beck CL, George AL Jr, Conte Camerino D. Aging-associated down-regulation of ClC-1 expression in skeletal muscle: phenotypic-independent relation to the decrease of chloride conductance. FEBS Lett 1999; 449: 12–16.

Ruben PC, Starkus JG, Rayner MD. Steady-state availability of sodium channels. Interactions between activation and slow inactivation. Biophys J 1992; 61: 941–55.

Ruff RL. Na current density at and away from endplates on rat fast- and slow-twitch skeletal muscle fibers. Am J Physiol 1992; 262: C229–34.

Ruff RL. Effects of temperature on slow and fast inactivation of rat skeletal muscle Na^+ channels. Am J Physiol 1999; 277: C937–47.

Ruff RL, Lennon VA. End-plate voltage-gated sodium channels are lost in clinical and experimental myasthenia gravis. Ann Neurol 1998; 43: 370–9.

Ruff RL, Whittlesey D. Na^+ currents near and away from endplates on human fast and slow twitch muscle fibers. Muscle Nerve 1993a; 16: 922–9.

Ruff RL, Whittlesey D. Comparison of Na^+ currents from type IIa and IIb human intercostal muscle fibers. Am J Physiol 1993b; 265: C171–7.

Ruff RL, Simoncini L, Stuhmer W. Comparison between slow sodium channel inactivation in rat slow- and fast-twitch muscle. J Physiol (Lond) 1987; 383: 339–48.

Sakmann B, Neher E. Geometric parameters of pipettes and membrane patches. In: Sakmann B, Neher E, editors. Single channel recording. New York: Plenum Press, 1983. p. 37–51.

Sashihara S, Greer CA, Oh Y, Waxman SG. Cell-specific differential expression of Na^+ channel beta1-subunit mRNA in the olfactory system during postnatal development and after denervation. J Neurosci 1996; 16: 702–13.

Schiaffino S, Reggiani C. Molecular diversity of myofibrillar proteins: gene regulation and functional significance. [Review]. Physiol Rev 1996; 76: 371–423.

Simoncini L, Stühmer W. Slow sodium channel inactivation in rat fast-twitch muscle. J Physiol (Lond) 1987; 383: 327–37.

Stein TP, Schluter MD, Moldawer LL. Endocrine relationships during human spaceflight. Am J Physiol 1999; 276: E155–62.

Struyk AF, Scoggan KA, Bulman DE, Cannon SC. The human skeletal muscle Na channel mutation R669H associated with hypokalemic periodic paralysis enhances slow inactivation. J Neurosci 2000; 20: 8610–7.

Talmadge RJ. Myosin heavy chain isoform expression following reduced neuromuscular activity: potential regulatory mechanisms. [Review]. Muscle Nerve 2000; 23: 661–79.

Todt H, Dudley SC Jr, Kyle JW, French RJ, Fozzard HA. Ultra-slow inactivation in μ1 Na^+ channels is produced by a structural rearrangement of the outer vestibule. Biophys J 1999; 76: 1335–45.

Townsend C, Horn R. Effect of alkali metal cations on slow inactivation of cardiac Na^+ channels. J Gen Physiol 1997; 110: 23–33.

Trimmer JS, Cooperman SS, Tomiko SA, Zhou JY, Crean SM, Boyle MB, et al. Primary structure and functional expression of a mammalian skeletal muscle sodium channel. Neuron 1989; 3: 33–49.

Vedantham V, Cannon SC. Slow inactivation does not affect movement of the fast inactivation gate in voltage-gated Na^+ channels. J Gen Physiol 1998; 111: 83–93.

Vilin YY, Makita N, George AL Jr, Ruben PC. Structural determinants of slow inactivation in human cardiac and skeletal muscle sodium channels. Biophys J 1999; 77: 1384–93.

Waxman SG. The neuron as a dynamic electrogenic machine: modulation of sodium-channel expression as a basis for functional plasticity in neurons. [Review]. Philos Trans R Soc Lond B Biol Sci 2000; 355: 199–213.

Wheeler MT, Snyder EC, Patterson MN, Swoap SJ. An E-box within the MHC IIB gene is bound by MyoD and is required for gene expression in fast muscle. Am J Physiol 1999; 276: C1069–78.

Wood SJ, Slater CR. Action potential generation in rat slow- and fast-twitch muscles. J Physiol (Lond) 1995; 486: 401–10.

Yanagita T, Kobayashi H, Yamamoto R, Takami Y, Yokoo H, Yuhi T, et al. Protein kinase C and the opposite regulation of sodium channel alpha- and beta1-subunit mRNA levels in adrenal chromaffin cells. J Neurochem 1999; 73: 1749–57.

Yang JS, Sladky JT, Kallen RG, Barchi RL. TTX-sensitive and TTX-insensitive sodium channel mRNA transcripts are independently regulated in adult skeletal muscle after denervation. Neuron 1991; 7: 421–7.

Yang JS, Bennett PB, Makita N, George AL, Barchi RL. Expression of the sodium channel β_1 subunit in rat skeletal muscle is selectively associated with the tetrodotoxin-sensitive α subunit isoform. Neuron 1993; 11: 915–22.

Received June 28, 2000. Revised December 14, 2000.
Accepted February 1, 2001